Spatio-spectral Wiener Estimation from Multispectral Images Recorded under Fluorescent Illumination

Yuri Murakami, Ken Fukura, Masahiro Yamaguchi and Nagaaki Ohyama

Imaging Science & Engineering Laboratory, Tokyo Institute of Technology

Abstract

When multispectral images are recorded under fluorescent illumination with insufficient power, sometimes color estimation error as well as noise increase in the reproduced color images. This is because some of the band images gain only low S/N ratio under fluorescent illumination. To improve the image fidelity, this paper proposes to combine spatial restoration methods with color image reproduction. Several methods including spatio-spectral Wiener estimation are examined through simulations. As a result, it is confirmed that spatio-spectral Wiener estimation reduces color estimation error and noise without visually-perceived degradation of spatial resolution.

Introduction

Though multispectral imaging realizes high fidelity color reproduction [1-4], the expected accuracy cannot be obtained when an image is captured under fluorescent illumination with insufficient power. Except for line spectra, the spectral power of fluorescent lamps is low. Thus, when narrow band color filters of multispectral camera are used, some specific band images become very dark; that is, their S/N ratio becomes low. As a result, as well as reducing color estimation accuracy, noise becomes obvious in the reproduced images. There is no need to seriously consider such problems for conventional three-channel cameras because their color filters have wide spectral bands.

In order to reduce noise on the recorded multispectral images, image restoration method such as spatial averaging operator can be effective. There are two simple ways to apply restoration methods to multispectral-image-based color reproduction: applying it before and after color estimation procedure. In addition, we can think about combining spatial restoration and color estimation to work as a single operation. In this paper, these different approaches are compared from the viewpoint of image fidelity improving when multispectral images are recorded under fluorescent illumination.

In this paper, we assume that color estimation is performed based on spectral reflectance estimation by Wiener estimation. In addition, spatial Wiener filtering [5] is employed for image restoration, which is one of the effective methods of restoring images in the presence of noise. Though the both terms, Wiener estimation and Wiener filtering, are used conventionally, they are derived based on the same criteria. Therefore we can simply combine them into a spatio-spectral Wiener estimation, which can be more effective than applying them separately.

Figure 1 shows four different approaches to obtain a color image from a multispectral image. The first one referred to as '1D' is a conventional method, in which spectral reflectance is estimated by pixel-by-pixel Wiener estimation and the color is calculated from the estimated spectral reflectance. The next one referred to as '1D+2D' consists of a color estimation followed by a two-dimensional spatial Wiener filtering. On the other hand, '2D+1D' consists of a spatial Wiener filtering followed by a color image estimation. The last one referred to as '3D' corresponds to a three-dimensional spatio-spectral Wiener estimation.

In this paper, for the purpose of improving the reproduced image quality when multispectral images are recorded under fluorescent illumination, the effectiveness of the above-mentioned four approaches is examined. Since Wiener filtering is a kind of spatial averaging operators, it involves the degradation of spatial resolution. Therefore the degradation in spatial resolution is also evaluated.

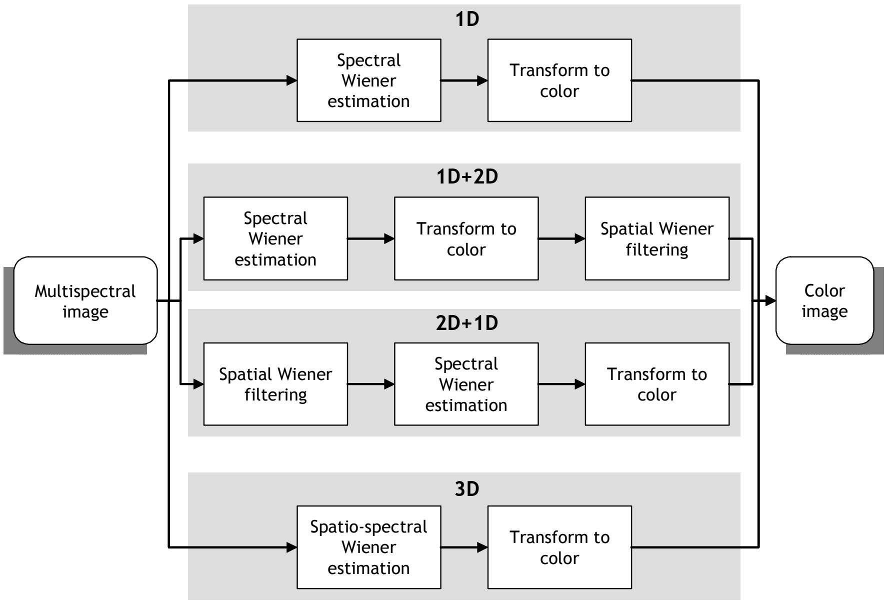

Figure 1. Block diagram of four color estimation methods accompanied with image restoring.

Spatio-spectral Wiener estimation

This section describes spatio-spectral Wiener estimation as well as other spectrum estimation methods accompanied with image restoring.

Spectral Wiener estimation (1D)

Let us start with the conventional Wiener estimation of spectral reflectance **f** from multispectral image data **g**, where we focus on the estimation related to just one pixel. Assuming that the number of color channels of multispectral images is *N*, **g** is an *N*-dimensional column vector. The relation between them can be written as

$$\mathbf{g} = \mathbf{Hf} + \mathbf{n}\,, \qquad (1)$$

where **H** is a system matrix that consists of the spectral sensitivity of the camera and the illumination spectrum, and **n** is a noise. A linear estimation is given by

$$\hat{\mathbf{f}} = \mathbf{Ag}\,, \qquad (2)$$

where **A** is an estimation matrix. In the case of Wiener estimation, **A** is given by

$$\begin{aligned}\mathbf{A} &= \left\langle \mathbf{fg}^T \right\rangle \left\langle \mathbf{gg}^T \right\rangle^{-1} \\ &= \left\langle \mathbf{ff}^T \right\rangle \mathbf{H}^T \left(\mathbf{H} \left\langle \mathbf{ff}^T \right\rangle \mathbf{H}^T + \left\langle \mathbf{nn}^T \right\rangle \right)^{-1}\end{aligned}, \qquad (3)$$

where <> is ensemble averaging operator. To derive the matrix **A**, the correlation matricies $\left\langle \mathbf{ff}^T \right\rangle$ and $\left\langle \mathbf{nn}^T \right\rangle$ are required.

1	2	3	4	5
6	7	8	9	10
11	12	13	14	15
16	17	18	19	20
21	22	23	24	25

Figure 2. Pixel index in the window

Spatial Wiener filtering & Spectral Wiener estimation (2D+1D/1D+2D)

Consider a rectangle window in an image, which consists of $25(=5\times5)$ pixels for instance. Assuming that an original image of the window **x** is degraded by only an additive noise $\boldsymbol{\eta}$, the degraded image **y** is written by

$$\mathbf{y} = \mathbf{x} + \boldsymbol{\eta}\,, \qquad (4)$$

where **x**, **y** and $\boldsymbol{\eta}$ are 25-dimensional column vectors and they are in raster-scanning notation as shown in fig. 2. The central pixel of the restored image is given by

$$\hat{x}_{13} = \mathbf{b}^T \mathbf{y}\,, \qquad (5)$$

where **b** is a restoring filter. If we consider a spatially invariant filter, the whole image is restored by scanning with a single filter. In the case of Wiener filter, **b** is given by

$$\mathbf{b}^T = \left\langle x_{13}\mathbf{x}^T \right\rangle \left\langle \mathbf{y}\mathbf{y}^T \right\rangle = \left\langle x_{13}\mathbf{x}^T \right\rangle \left(\left\langle \mathbf{x}\mathbf{x}^T \right\rangle + \left\langle \boldsymbol{\eta}\boldsymbol{\eta}^T \right\rangle \right)^{-1}, \quad (6)$$

where $\left\langle \mathbf{x}\mathbf{x}^T \right\rangle$ means the spatial correlation of the image and $\left\langle x_{13}\mathbf{x}^T \right\rangle$ is the central row of $\left\langle \mathbf{x}\mathbf{x}^T \right\rangle$.

In the case of Wiener filtering before color estimation, the following procedure is required. Let g_i^k and n_i^k be k-th elements of **g** and **n** of i-th pixel of the window. Put

$$\begin{cases} \tilde{\mathbf{g}}_k = \left(g_1^k, g_2^k, \cdots, g_{25}^k\right)^T \\ \tilde{\mathbf{n}}_k = \left(n_1^k, n_2^k, \cdots, n_{25}^k\right)^T \end{cases}, \quad (7)$$

where $\tilde{\mathbf{g}}_k$ is k-th multispectral image of the window and $\tilde{\mathbf{n}}_k$ is the related noise. Applying eqs. (5) and (6) as

$$\tilde{\mathbf{g}}_k \Rightarrow \mathbf{y}, \quad \tilde{\mathbf{n}}_k \Rightarrow \boldsymbol{\eta}, \quad (\tilde{\mathbf{g}}_k - \tilde{\mathbf{n}}_k) \Rightarrow \mathbf{x}, \quad (8)$$

we have the restored k-th multispectral image. After applying Wiener filtering to all channel images, spectral reflectance is estimated from the restored multispectral image by eqs. (2) and (3). In the derivation of matrix **A**, the correlation of the noise should be modified because the noise statistics on the restored multispectral image is different from that of the original multispectral image. The new statistics can be estimated as below. The restored k-th channel image is

$$\hat{g}_{13}^k = \mathbf{b}^T \tilde{\mathbf{g}}_k = \mathbf{b}^T (\tilde{\mathbf{g}}_k - \tilde{\mathbf{n}}_k) + \mathbf{b}^T \tilde{\mathbf{n}}_k, \quad (9)$$

where $(\tilde{\mathbf{g}}_k - \tilde{\mathbf{n}}_k)$ represents an ideal image without noise, $\mathbf{b}^T (\tilde{\mathbf{g}}_k - \tilde{\mathbf{n}}_k)$ represents the filtered (sometimes blurred) ideal image, and $\mathbf{b}^T \tilde{\mathbf{n}}_k$ is the noise on the restored image. If the noise variance of the original k-th channel image is $\gamma_k{}^2$, the noise variance of the restored image becomes

$$\left\langle \left(\mathbf{b}^T \tilde{\mathbf{n}}_k\right)^2 \right\rangle = \mathbf{b} \left\langle \tilde{\mathbf{n}}_k \tilde{\mathbf{n}}_k{}^T \right\rangle \mathbf{b}^T = \gamma_k{}^2 \|\mathbf{b}\|^2, \quad (10)$$

which is used in the derivation of **A**. Generally, most coefficients of **b** is positive and the sum of the coefficients is equal to 1, which results in $\|\mathbf{b}\|^2 < 1$. This means noise is reduced in the restored multispectral images.

The next is the case of Wiener filtering after color estimation. Though the detail equations are omitted because of space limitations, the outline is the following. A spectral reflectance image is estimated from multispectral image pixel by pixel by eqs. (5) and (6). Then it is transformed to a color image as XYZ, L*a*b*, RGB and so on. After that, the color image is restored by spatial Wiener filtering by applying eqs. (5) and (6). Though any color space can be used for Wiener filtering, the noise estimation of the color image becomes difficult when nonlinear color spaces are selected such as L*a*b*.

Spatio-spectral Wiener estimation (3D)

Three column vectors are defined for a window as

$$\mathbf{F} = \begin{pmatrix} \mathbf{f}_1 \\ \mathbf{f}_2 \\ \vdots \\ \mathbf{f}_{25} \end{pmatrix}, \quad \mathbf{G} = \begin{pmatrix} \mathbf{g}_1 \\ \mathbf{g}_2 \\ \vdots \\ \mathbf{g}_{25} \end{pmatrix}, \quad \mathbf{N} = \begin{pmatrix} \mathbf{n}_1 \\ \mathbf{n}_2 \\ \vdots \\ \mathbf{n}_{25} \end{pmatrix}, \quad (11)$$

where the subscript is a pixel index of the window. Using these notations, eq.(1) is rewritten by

$$\mathbf{G} = (\mathbf{I} \otimes \mathbf{H})\mathbf{F} + \mathbf{N}, \quad (12)$$

where $\otimes$ is Kronecker product and **I** is a 25×25 identity matrix. The spectral reflectance of the central pixel is estimated by

$$\hat{\mathbf{f}}_{13} = \mathbf{C}\mathbf{G}, \quad (13)$$

where **C** is a matrix to estimate $\mathbf{f}_{13}$ from all multispectral image signals inside the window. In the case of Wiener estimation, **C** is given by

$$\mathbf{C} = \left\langle \mathbf{f}_{13}\mathbf{G}^T \right\rangle \left\langle \mathbf{G}\mathbf{G}^T \right\rangle^{-1} = \left\langle \mathbf{f}_{13}\mathbf{F}^T \right\rangle (\mathbf{I} \otimes \mathbf{H})^T \left((\mathbf{I} \otimes \mathbf{H}) \left\langle \mathbf{F}\mathbf{F}^T \right\rangle (\mathbf{I} \otimes \mathbf{H})^T + \left\langle \mathbf{N}\mathbf{N}^T \right\rangle \right)^{-1} \quad (14)$$

To calculate matrix **C**, we need an inverse matrix of the dimension of $25N \times 25N$. When the number of color channels is 6, for instance, the dimension becomes 150×150, which is quite a large number.

To modify the matrix **C** in more useful form, we introduce an assumption that the correlation between elements of **F** is separable into the product of spatial and spectral correlation; then the correlation matrix of **F** can be expressed as

$$\left\langle \mathbf{F}\mathbf{F}^T \right\rangle = \left\langle \overline{\mathbf{x}\mathbf{x}}^T \right\rangle \otimes \left\langle \mathbf{f}\mathbf{f}^T \right\rangle, \quad (15)$$

where $\left\langle \overline{\mathbf{x}\mathbf{x}}^T \right\rangle$ is the normalized spatial correlation matrix with 25×25 dimensions. Furthermore, the correlation matrices are expressed by singular value decomposition (SVD) as

$$\left\langle \tilde{\mathbf{x}}\tilde{\mathbf{x}}^T \right\rangle = \mathbf{U}\Omega^2\mathbf{U}^T , \qquad (16)$$

$$\mathbf{H}\left\langle \mathbf{f}\mathbf{f}^T \right\rangle \mathbf{H}^T = \mathbf{V}\Lambda^2\mathbf{V}^T , \qquad (17)$$

where **U** and **V** are unitary matrices and Ω^2 and Λ^2 are diagonal matrices. Assuming random white noise,

$$\left\langle \mathbf{N}\mathbf{N}^T \right\rangle = \Gamma^2 = \begin{pmatrix} \gamma^2 & & \mathbf{0} \\ & \ddots & \\ \mathbf{0} & & \gamma^2 \end{pmatrix}, \qquad (18)$$

we have

$$\mathbf{C} = \left[\left(\mathbf{e}^T \mathbf{U}\Omega^2 \right) \otimes \left(\left\langle \mathbf{f}\mathbf{f}^T \right\rangle \mathbf{H}^T \mathbf{V}^T \right) \right] \left(\Omega^2 \otimes \Lambda^2 + \Gamma^2 \right)^{-1} \left(\mathbf{U}^T \otimes \mathbf{V}^T \right), \qquad (19)$$

where $\mathbf{e}^T = (0 \ \cdots \ 0 \ 1 \ 0 \ \cdots \ 0)$. To calculate matrix **C**, we need SVD calculations of 25×25 matrix and $N \times N$ matrix instead of the inverse calculation of $25N \times 25N$ matrix.

Evaluation measures

Color estimation accuracy

We assume a virtual object consisting of 24 uniform regions with the spectral reflectance of Macbeth ColorChecker as shown in fig.3. One color region consists of 100×100 pixels and the whole image consists of 400×600 pixels. Using this spectral reflectance image, color estimation simulation is done and estimated L*a*b* image is obtained. For this image, a measure for color estimation accuracy ΔE is defined by

$$\Delta E = \frac{1}{24} \sum_{j=1}^{24} \Delta E_j , \qquad (20)$$

where ΔE_j is ΔE^*_{ab} of the average L*a*b* of the central 96×96 pixels of *j*-th color region.

Noise

The same virtual object is used for noise evaluation. A measure σ_l (l=L^*, a^* or b^*) is defined by

$$\sigma_l = \sqrt{\frac{1}{24} \sum_{j=1}^{24} \left(\sigma_j^l \right)^2} , \qquad (21)$$

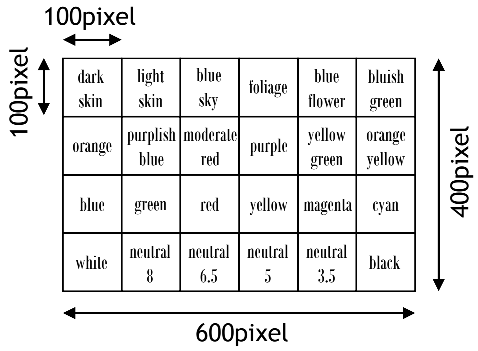

Figure 3. Virtual object consisting of the spectral reflectance functions of Macbeth ColorChecker

where σ_j^l is the standard deviation of the central 96×96 pixels of *j*-th color region in the estimated L*, a* or b* image.

Spatial resolution

We assume a virtual object consisting of 1-pixel-width white linear object on dark background; (L^*, a^*, b^*) of the white object and the background are (100, 0, 0) and (10, 0, 0) respectively. The color estimation simulation is performed and the average profile is obtained from the estimated L* image. If there is no degradation of spatial resolution, the profile has the peak with 100 on 10 background. However, when the estimated image includes some blur, the peak value declines from 100 and the neighbor-pixel value is raised from 10. In this paper, instead of the profile itself, the only peak value of the average profile is used as a measure of spatial resolution, which is referred to as L_{Peak}.

Color image reproduction of natural scene

The color estimation simulation is also done for natural scene and the image fidelity is evaluated. For this purpose, two 512-pixel-square spectral reflectance images, 'Toy' and 'Scarf', are prepared, which are estimated from 16-band images captured by a 16-band camera [6].

Simulation Results

Conditions

Simulated multispectral images are calculated based on the spectral sensitivity of a six-band HDTV video camera [7], where the recording illumination is

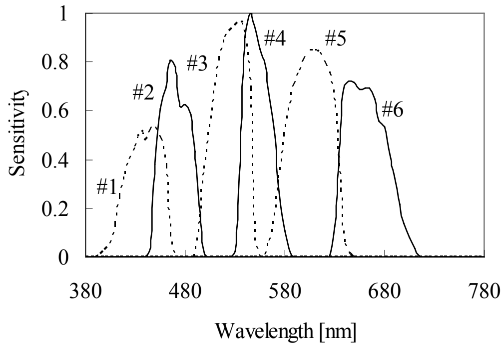

Figure 4. Spectral sensitivity of six-band video camera used in the simulation

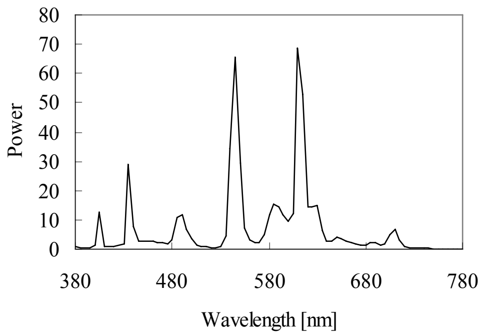

Figure 5. Spectral power distribution of fluorescent lamp F12

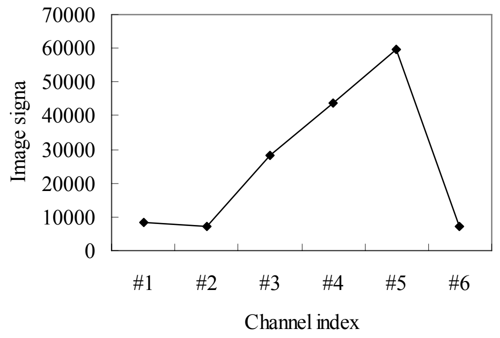

Figure 6. Six-band image signal of white object under F12.

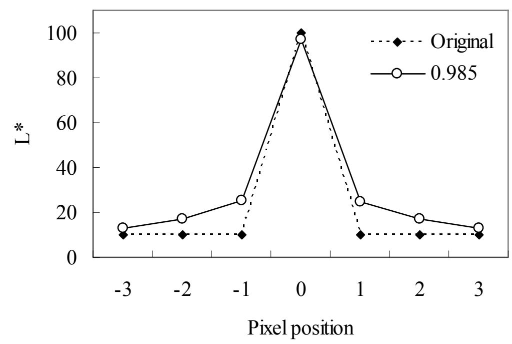

Figure 7. Average profile of the 1-pixel width white linear object estimated with 2D+1D at ρ=0.985

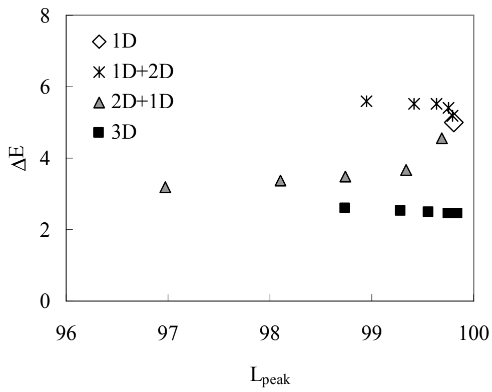

Figure 8. ΔE vs L_{peak}

assumed to be fluorescent lamp F12. Their spectral characteristics are shown in figs. 4 and 5. Gaussian random white noise is added to the image data at PSNR (peak signal to noise ratio) =40 dB.

The correlation of spectral reflectance is made from 24 spectral reflectance functions of Macbeth ColorChecker. The spatial correlation is formed assuming that the sequence of image pixels is Markov sequence [5], which means the whole correlation matrix is defined by a single correlation coefficient ρ. These correlation matrices are used through the following simulations.

The following four methods are compared.

1D: conventional pixel-by-pixel spectral Wiener estimation.

1D+2D: pixel-by-pixel spectral Wiener estimation followed by spatial Wiener filtering

2D+1D: spatial Wiener filtering of multispectral image followed by spectral Wiener estimation

3D: spatio-spectral Wiener estimation.

Results

Figure 6 shows the 6-band image signals of a white object. We can see that the signals of #1, #2 and #6 are far lower than the other three channels.

Figure 7 shows an example of the profiles for the evaluation of spatial resolution, where the estimation is done with 2D+1D at ρ=0.985. We can see that the profile is widened and the peak value is slightly reduced: L_{peak}=96.97. Though any formal subjective

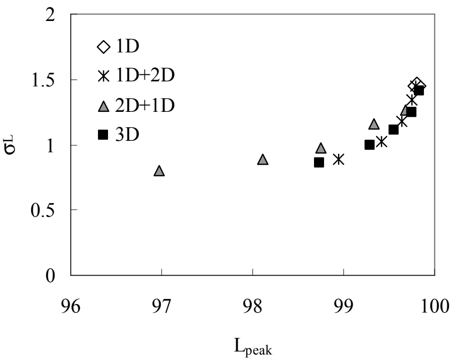

Figure 9. σ_L vs L_{peak}

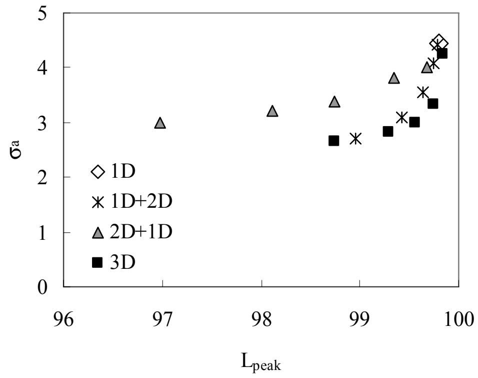

Figure 10. σ_a vs L_{peak}

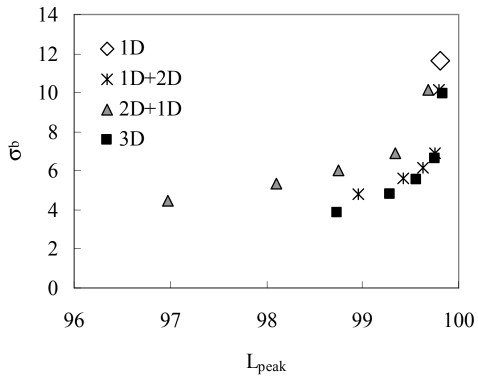

Figure 11. σ_b vs L_{peak}

evaluation has not been done, we found that the degradation can be negligible in L_{peak}>99 through some rough visual observations.

Figure 8 shows ΔE vs. L_{peak} for four estimation methods. Five plots for each method except for 1D is related to the five spatial correlation coefficients ρ=0.6, 0.9, 0.95, 0.97, 0.985, which are ordered from right to left. Since a higher L_{peak} means higher spatial resolution, the plot on the bottom-right corner is desirable. We can see that 2D+1D reduces ΔE as ρ increases, which is accompanied with the reduction of L_{peak} though. On the other hand, 3D reduces ΔE without the degradation in spatial resolution. The error of 1D+2D is slightly higher than 1D, which is because Wiener filtering is operated in XYZ color space in spite of L*a*b* color space. If we apply Wiener filtering to the estimated L*a*b* image, the every error of 1D+2D is equal to the error of 1D in principle.

Figures 9-11 show σ_l (l=L*, a* or b*) vs L_{peak}, where the display format is the same as fig. 7. It is commonly observed that σ_l becomes lower as L_{peak} becomes lower. Furthermore, the plots of 1D+2D and 3D are almost overlapped and lay on the lower right-hand of 2D+1D plots. This means 1D+2D and 3D reduce noise more than 2D+1D at the same spatial resolution.

The results around L_{peak}=99.3 are extracted and shown in table 1, where each parameter ρ is also indicated. Table 1 shows that 3D reduces ΔE and σ_b in almost half of those of 1D. We can see that 1D+2D

Table 1. ΔE, σ_L, σ_a, σ_b for the virtual Macbeth image at around L_{peak}=99.3

	ΔE	σ_L	σ_a	σ_b	ρ
1D	4.99	1.45	4.45	11.65	-
1D+2D	5.54	1.02	3.08	5.60	0.97
2D+1D	3.66	1.16	3.82	6.89	0.9
3D	2.52	1.00	2.84	4.77	0.97

Table 2. Average and maximum ΔE^*_{ab} of images 'Toy' and 'Scarf'

	Toy		Scarf		
ΔE^*_{ab}	Ave	Max	Ave	Max	ρ
1D	12.77	82.11	8.93	70.15	-
1D+2D	9.97	61.72	6.47	54.21	0.97
2D+1D	10.10	66.70	6.70	58.33	0.9
3D	8.45	67.79	5.66	62.15	0.97

reduces noise but does not reduce color error. On the other hand, 2D+1D reduces color error but the reduction of noise is smaller than the others.

Table 2 is the average and the maximum ΔE^*_{ab} for the images ‘Toy’ and ‘Scarf’. The same spatial correlation parameter is used in the results of table 1, which means the spatial degradations are almost same among three methods and it is visually negligible. Though 3D reduces the average error for both images, the reduction is smaller than the results of the virtual Macbeth of table 1. This is because natural images include less uniform regions than Macbeth image, even if the spatial correlation is high.

Figure 12 shows a 135-pixel-squre region of blue channel image of ‘Scarf’ in sRGB. We can see that noise on 1D-reconstruction image is reduced by all 1D+2D, 2D+1D and 3D in the right-hand relatively uniform region. Focusing on the lines on the angel’s feather in the bottom left corner, we can recognize the lines in only 3D-reconstruction image. The results show that 3D reduces noise with the minimal distortion of spatial resolution.

Complemental results

All above simulations are done under the assumption of F12 recording illumination and PSNR=40dB. This final section mentions the results in the other conditions.

When D65 is used as a recording illumination at PSNR=40dB, though average ΔE^*_{ab} is slightly improved by applying 3D, the difference between 1D and 3D are almost invisible in the reproduced color images. On the other hand, in the case of noise free, the results of four methods become completely same, which can be explained from the equations themselves. Besides, there is no degradation of spatial resolution in this case.

Conclusions

This paper examined several spectrum estimation methods accompanied by image restoration, including spatio-spectral Wiener estimation. Through the simulations with 6-band camera and F12 recording illumination, it is confirmed that spatio-spectral Wiener estimation most effectively reduces color estimation error as well as noise. Without

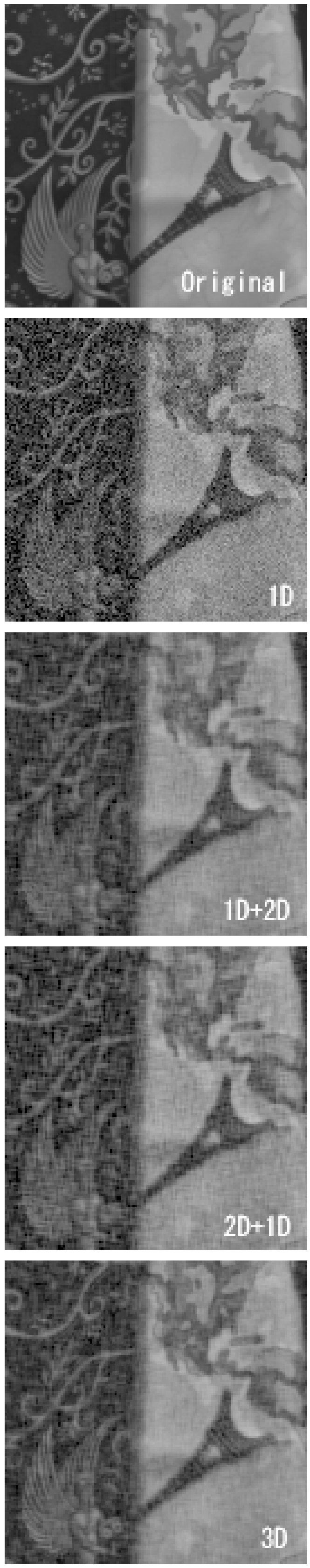

Figure 12. 135-pixel-square region of blue channel image of ‘Scarf’ in sRGB.

visually-perceived degradation of spatial resolution, average ΔE_{ab}^{*} is reduced to almost 2/3 and the noise is far reduced compared to the conventional pixel-by-pixel approach.

References

1. B. Hill, Color capture, color management and the problem of metamerism, Proc. SPIE 3963, 3-14 (2000).
2. H. Haneishi, T. Hasegawa, A. Hosoi, Y. Yokoyama, N. Tsumura and Y. Miyake, “System design for accurately estimating spectral reflectance of art paintings,” Appl. Opt. 39(35) 6621-6632 (2000).
3. M. Yamaguchi, T. Teraji, et. al., Color image reproduction based on the multispectral and multiprimary imaging: Experimental evaluation, Proc. SPIE, 4663, 15-26 (2002).
4. M. Yamaguchi, H. Hideaki, H. Fukuda, J. Koshimoto, H. Kanazawa, M. Tsuchida, R. Iwama, and N. Ohyama, High-fidelity video and still-image communication based on spectral information: Natural Vision system and its applications, Proc. SPIE 6062, (2006).
5. A. K. Jain, Fundam entals of digital image processing, Prentice-Hall, Inc., 276-279 (Wiener filtering) and 33-34 (Markov process) (1989).
6. H. Fukuda, T. Uchiyama, H. Haneishi, M. Yamaguchi and N. Ohyama, Development of 16-band multispectral image archiving system, Proc. SPIE 5667, 136-145 (2002).
7. K. Ohsawa, T. Ajito, H. Fukuda, H. Haneishi, M. Yamaguchi and N. Ohyama, Sic-band HDTV camera system for spectrum-based color reproduction, J. Img. Sci. and Tech., 48(2), 85-92 (2004).